

Chapter 3

Screening of antifungal actinomycetes against fungal phytopathogens of *Cajanus* *cajan*



Chapter-3

3 Screening of antifungal actinomycetes against fungal phytopathogens of *Cajanus cajan*

3.1 Introduction

Modern plant-fungal management necessitates the development of innovative chemotherapeutic agents with a distinct mode of action and chemical structure from existing fungicides. Problems with fungicide resistance, which lead to high application rates of many synthetic fungicides and negative impacts on the environment, are the primary cause of these requests (Cohen & Coffey, 1986; Früh et al., 1996; Knight et al., 1997). Since Waksman's initial systematic screening programmes for antimicrobial metabolites in the 1940s, microbial cultures have been a key source of antibiotic compounds (Okami, 1988). Actinomycetes are among the most desirable sources of antibiotics and other physiologically active chemicals with a high commercial value, including vitamins, alkaloids, plant growth factors, enzymes, and enzyme inhibitors (Omura, 1986). It is well-established that they can parasitize and destroy the spores of fungal plant pathogens (El-Tarabily et al., 1997). Creating extracellular hydrolytic enzymes can metabolize numerous substances, including sugars, alcohols, amino acids, and aromatic molecules. Their metabolic variety results from their extraordinarily vast genome, which contains hundreds of transcription factors that regulate gene expression, allowing them to respond to particular needs (Kohei et al., 2002).

Pigeon pea (*Cajanus cajan* (L) Millsp.) is an important food legume cultivated in semi-arid tropical and sub-tropical farming systems under diverse agro-ecological conditions (Bekele-Tesemma, 2007). It offers humans high-quality vegetable protein and is a source of animal feed and firewood. It is only cultivated in developing nations, primarily in Asia and Africa. In 2007, the crop was grown over 4.6 million hectares, according to FAO statistics (FAO, 2008). Approximately ninety percent of its output comes from South Asia and Southeast Asia, and 73% of the world's pigeon pea production comes from India (Pais & Bansal, 2019). Pigeon pea's most devastating disease is Fusarium wilt. The annual loss in India and eastern Africa owing to pigeonpea wilt was estimated to be 71 million and 5 million US dollars, respectively (Gohel et al., 2006; Gwata et al., 2006; Raju et al., 1999; Reddy et al., 1990). The pathogen is soil-borne, and chemical management in established cases is unrealistic. In addition, the increased usage of

synthetic substances to increase crop yield and disease management is a rising cause for worry. Chemical fungicides such as Thiram, Bavistin, and Benomyl are commonly used to manage Fusarium wilt (Meena et al., 2002; Melent'ev et al., 2006; Vidhyasekaran et al., 1997).

As biological control agents, beneficial microbes have increasingly become the focus of scientists in recent years due to their economic and environmental benefits (Jing et al., 2020; Qi et al., 2019; Wei et al., 2020). Numerous microbial species have been identified as biocontrol agents, including *Bacillus spp.*, *Burkholderia spp.*, *Pseudomonas spp.*, *Rhizobium spp.*, and *Stenotrophomonas spp.*, among others (Bubici et al., 2019). *Streptomyces*, in particular, can build a symbiotic connection with plants to encourage the host's growth and produce a variety of chemicals that hinder the infection of pathogens (Chen et al., 2018; van Bergeijk et al., 2020; van der Heul et al., 2018). 1–20% of the culturable soil microorganisms are *Streptomyces*, related to actinomycetes (Olanrewaju & Babalola, 2019). Among the bioactive compounds produced are those with antibacterial, antiviral, and anticancer properties (van Bergeijk et al., 2020). Actinomycetes are the source of around two-thirds of all-natural antibiotics, with the *Streptomyces* genus accounting for about seventy-five percent (Franco-Correa et al., 2010). They are the predominant organisms used by the pharmaceutical industry to manufacture antibiotics (Olanrewaju & Babalola, 2019).

The first and most crucial stage in turning putative biological control agents into viable commercial solutions is screening. BCAs may act through a variety of mechanisms; therefore, when screening for ACC, different possible actions should be evaluated (Compant et al., 2005). Antibiosis is the most successful and widespread biocontrol strategy employed by biocontrol agents (Haggag & Mohamed, 2007). Antibiosis is mainly obtained by inducing fungal enzymes that break down cell walls, termed mycolytic enzymes or secondary antifungal metabolites (Podile & Kishore, 2007). Several PGPR inoculants are being marketed as phytohormone producers, plant growth boosters for improved nutrient uptake, or biocontrol agents to suppress plant disease (bioprotectants) (biostimulants). Bacteria belonging to the genera, *Streptomyces*, *Pseudomonas*, and *Agrobacterium* are the most extensively researched and increasingly marketed biological control agents. To suppress plant disease, at least one mechanism is used, such as the production of Siderophores or antibiotics as well as the development of systemic resistance. (Figueiredo et al., 2010). Han et al. (2005) showed that the HR4 strain of *Delftia tsuruhatensis* inhibited the

growth of a variety of plant diseases, including *Pyricularia oryzae*, *Rhizoctonia solani*, and *Xanthomonas oryzae*. Urban and agricultural wastes containing microbial antagonists are the most efficient method for reducing avocado and citrus root infections (Sultana et al., 2006).

3.2 Materials and methods

3.2.1 Screening of actinomycetes

Fusarium udum and *Streptomyces* sp. S-9 were cultured for seven days at 28°C on PDA medium. In the centre of the plate, an 8-mm-diameter sterile cork borer was used to create an 8-mm-diameter agar block containing an indicator fungus. 10 mm from the edge of the agar block, inoculate it with a single colony of actinomycetes (Bredholdt et al., 2007). After seven days of incubation at 28°C, mycelial growth inhibition was determined (Bredholdt et al., 2007). Inhibition of mycelial development in response to the bacterial isolate was indicative of hostile behaviour. Ji et al. (2013) method was used to measure the proportion of inhibition of radial mycelial development as follows:

$$\text{Inhibition} = \frac{\text{Growth diameter in untreated control} - \text{Growth diameter in treatment}}{\text{Growth diameter in untreated control}} \times 100$$

3.2.2 Phenotypic characterization of *Streptomyces* sp.

Using scanning electron microscopy (JEOLJSM-6380 LV, Japan), the morphological properties of cultures grown on ISP-3 agar at 28 °C for two weeks were analysed (Jin et al., 2019). The SEM sample was obtained by cutting a block from the agar plate and immobilizing it in 2.5% glutaraldehyde buffer (pH 7.2) at 4 °C for about 1.5 h. Samples were dehydrated using a graded ethanol, passed through tertiary butanol, and then dried completely after two phosphate-buffered washes. The dried samples were mounted on a stub-bearing adhesive and gold-sputter-coated under vacuum (Guan et al., 2015).

3.2.3 Scanning electron microscopy (SEM)

Mycelia samples of *F. udum* were fixed in 4% glutaraldehyde at 4±1 °C overnight, then rinsed three times with 0.05 M Sodium cacodylate (Sigma Aldrich, USA) buffer (pH 7.2) for 10 minutes. The samples were then fixed with 1 percent osmium tetroxide (Sigma Aldrich, USA) at

4±1°C for two hours and briefly rinsed with distilled water. To ensure total dehydration, the hyphae were dehydrated in a series of ethanol concentrations (50, 70, 80, and 90 percent) for 10 minutes each, followed by 20 minutes in 100 percent ethanol. After that, the hyphae were put in isoamyl acetate. The samples were mounted on stubs and sputter-coated with gold-palladium before being inspected at 20 kV with a scanning electron microscope (Model- JEOLJSM-6380 LV, Japan).

3.2.4 Production and extraction of antifungal metabolites from S-9

3.2.4.1 Extraction

Actinomycetes were separately grown in tryptone yeast extract (ISP-1) medium at 28° C at 220 rpm for five days. The supernatant was obtained by centrifuging broth at 8000 rpm for 10 min. Then, an equal volume of ethyl acetate was added to the supernatant. The mixture was shaken vigorously for 1 h, and the ethyl acetate phase containing antibiotic/antifungal metabolites was separated from the aqueous phase. It was evaporated to dryness in a water bath, and the residue obtained was subjected to determine antimicrobial activity.

3.2.4.2 Determination of the antifungal activity of extract

During previous studies from our lab, strain S-9 showed a maximum zone of inhibition against *Fusarium udum* ITCC 3241 (Kapur et al., 2018; Solanki, 2013). The present study of antifungal activity was determined using a well-diffusion method for extracts from strain S-9 and positive controls, cycloheximide (Hi-media, Mumbai). Fungus plug was put at the three corners, and extract was put in the center of the Petri plate. After 48 hrs of incubation, the plates were examined for the inhibition of the growth of pathogenic strain in each well. To better visualize the results, 10µl of MTT stain (LobaChemie) with a 1mg/ml concentration was added to each well.

3.2.5 Identification and Purification of Bioactive Compounds

3.2.5.1 Thin Layer Chromatography of Extracts

Silica gel TLC plates (60 F254, 0.2mm Merck, Germany) were used to separate crude extract constituents. As the mobile phase for ethyl acetate extract, the dichloromethane: methanol (9:1)

solvent solution (SRL, Mumbai) was utilized. The plates were air-dried, viewed under UV light, and marked with various fractions.

3.2.5.2 Bioautography and Purification of Bioactive compounds

On the strain S-9 TLC plate, a soft agar medium containing log phase culture of *F. udum* ITCC 3241 (108 cfu/ml) was spread. These plates were incubated at 30°C for 48 hours. After 48 hours of incubation, 1mg/ml of MTT tetrazolium (SRL, Mumbai) was used to stain pathogenic stacked TLC plates, which were then incubated overnight at 30°C (Selvameenal et al., 2009; Solanki et al., 2015; Taddei et al., 2006). The formation of white inhibition zones (around specified fractions) against a purple backdrop was seen on plates. The R_f values of bioactive fractions were determined by comparing an identical TLC plate on which extracts had been run with bioautography with an identical TLC plate on which extracts had been run without bioautography. Bioautography-identified bioactive fractions were scraped with silica gel from identical S-9 TLC plates. The separation of bioactive metabolites from silica gel was accomplished by adding ethyl acetate to S-9 and then centrifuging at 8000 rpm. The dried supernatants containing purified bioactive chemicals were analysed by ¹H NMR/FTIR/LC-MS Q-TOF).

3.2.5.3 Structural Analysis of Compounds

3.2.5.3.1 LC-MS analysis

The system consisted of SUNFIRE C8250X4.65µm (Thermo Scientific, USA). The mobile phase contained 0.1% of formic acid (SRL, Mumbai) (solvent A) and acetonitrile (SRL, Mumbai) (solvent B). The pumping of the solvents was done at a flow rate of 0.3 ml/min. The initial conditions of solvent A and solvent B (9:1) were maintained for 2 min. The gradient was shifted from ratio of 7:3 in 4 min, to 3:7 in next 4 min, followed by increment to 1:9 in 3 min, where it was kept for 3 min. Consequently, the mobile phase was regulated to its starting concentration in 2 min and detained for another 2 min to maintain equilibration again, this process results in a total time of 20 min. The mass spectrometer was functioned via positive ion mode. Multiple reaction monitoring was set for detecting compounds.

3.2.5.3.2 Proton Nuclear Magnetic Resonance (¹H NMR) of purified bioactive compounds

In order to figure out the structure of bioactive compounds in the S-9 strain, ¹H NMR was used on the purified fraction (Igarashi et al., 2005; Maskey et al., 2006; Solanki et al., 2015). A Bruker Ultrashield 500 Plus TM spectrometer with a 5mmPABBO probe was used for ¹H NMR. Deuterated chloroform (CDCl₃) (SRL, Mumbai) was used as a solvent. At 500 MHz, chemical shifts and coupling constants were measured in parts per million (ppm, δ).

3.2.5.3.3 FTIR Analysis

The sample was dissolved in 5 ml of ethanol, and the spectra were obtained between the wavelengths of 200 and 800 nm. FTIR Spectrophotometer (Shimadzu, FTIR Affinity 1, Japan) was used to capture the IR spectra. They were taken from 400 to 4000 cm⁻¹ using a KBr pellet technique.

3.3 Results

3.3.1 Phenotypic characterization of *Streptomyces* sp. S-9

The morphology of a four-week-old S-9 culture cultivated in ISP 3 media suggested belonging to the *Streptomyces* genus. The S-9 strain was an aerobic gram-positive actinomycete that formed a well-developed, branching, and non-fragmented mycelial matrix, but no aerial mycelium (Figure 3.1). Individual non-motile oval spores (2 μm) were formed on the substrate mycelium.

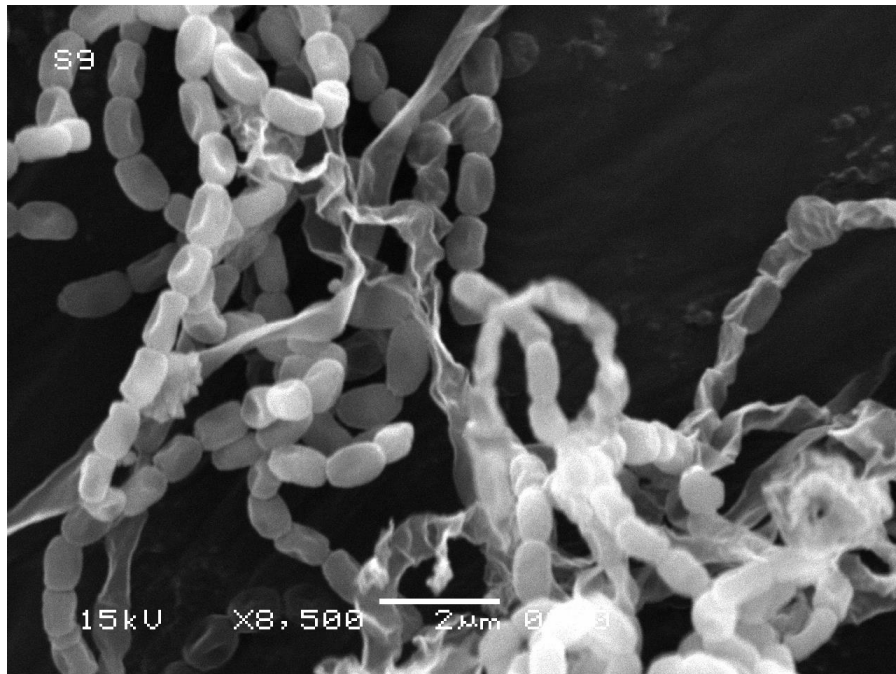


Figure 3.1: Scanning electron microscopy of strain S-9 grown on ISP 3 for 4 weeks at 28 °C
(Magnification = $\times 8,500$; Bar, 2.0 μm)

3.3.2 Effect of strain S-9 on *Fusarium udum* morphology

Figure 3.2 summarizes the SEM of pathogen-bacterial interactions during the antagonism assay. *Fusarium* pathogens impacted by *Streptomyces sp.* S-9 exhibited evident morphological changes, as detected by SEM image analysis of *F. udum* hyphae, according to the findings of the present investigation (Figure 3.2a-d). Less densely developed hyphae revealed normally long, cylindrical cells with a smooth exterior. As demonstrated in Figure 3.2, the test strain possessed fewer hyphae and degraded mycelia. The walls penetrated many places along the degenerated hyphae, forming small depressions. *F. udum* hyphae also deteriorated and contracted (Figs. 3.2b and d). As a biocontrol agent for Pigeon pea wilt diseases, the *Streptomyces sp.* strain S-9 exhibited excellent potential.

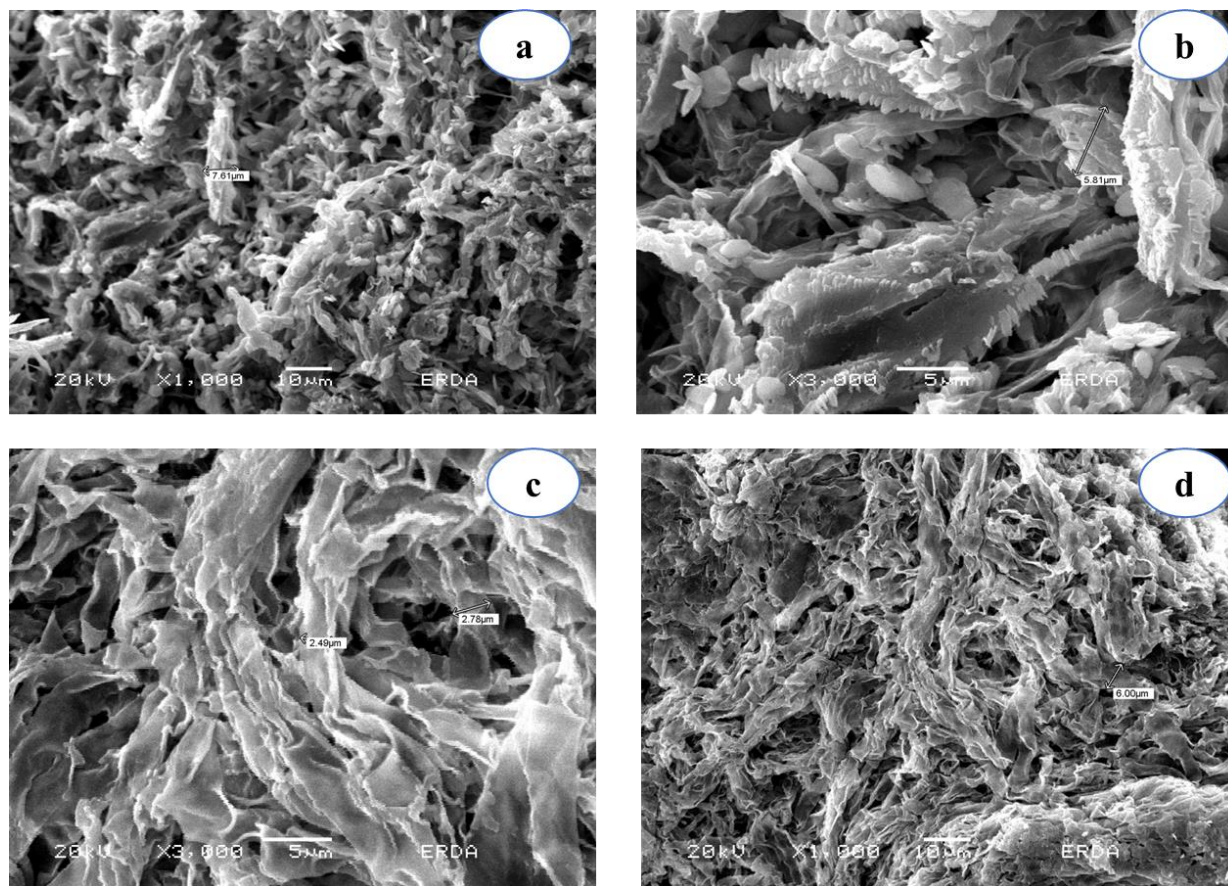


Figure 3.2: Scanning electron micrographs (SEM) of pathogen-bacterial interaction during antagonism assay against *F. udum* in dual culture. Images of *F. udum* from control plate (a and b); in dual culture with *Streptomyces* sp. S-9 (MK158952) (c and d). Mycelial abnormalities observed along with (a) Coagulation of cytoplasm, (b) mycelial shredding and shrinking, (c) leakage of cytoplasm and mycelial breakage, (d) Perforation, breakage, and shrinking, as compared to growth in the absence of antagonistic agent *Streptomyces* sp. S-9 (MK158952).

3.3.3 Bioautography and purification of bioactive compounds

Different bands were observed on TLC loaded with extract of S-9, and Rf value was calculated. A solvent system comprising ethyl acetate: chloroform: methanol (1: 1.5: 0.5) exhibited the best separation when compared to other solvent systems. Actinomycetes are known to produce compounds, but the ones that are biologically active need to be identified, and bioautography can help. Bioautography of strain S-9 extracts was carried out using immersion bioautography. As a result, just one bioactive molecule with an Rf value of 0.46 was found in strain S-9 (Figure 3.3).

Bioactive compounds identified by chromatographic techniques were isolated and purified. For ^1H NMR studies, powdered purified compounds were used instead of liquid samples.

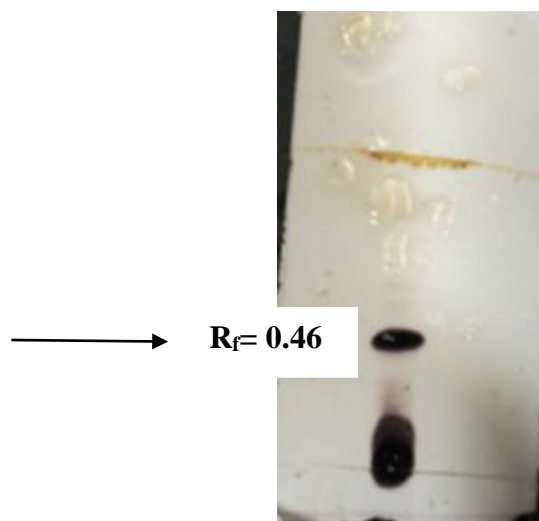


Figure 3.3: Bioactive fraction of S-9 ethyl acetate against *Fusarium udum*

3.3.4 LC-MS Analysis

Crude extracts/mixtures of natural products from strain *Streptomyces* sp. S-9 was subjected to LC-MS analysis to identify and characterize total bioactive compounds produced by these strains. LC-MS analysis at the positive mode of ethyl acetate extract of strain S-9 has been characterized based on their molecular ion (m/z) and fragment ion peaks (Table 3.1). The ethyl acetate extract's total ion chromatogram (TIC) exhibits six major peaks, excluding several minor peaks (Figure 3.4A&B). The LC peak observed at Positive ion Rt 25.08 min and Rt 15.44 min interval corresponded to the molecular ion peak at m/z 425.6 and 739.9 (Figures 3.5 & 3.6). In the negative ion, Rt 13.94 min and Rt 15.45 min interval corresponded to the molecular ion peak at m/z 784.0 and 783.9 (Figures 3.7 & 3.8). Using the calculated molecular weights of the identified compounds with prominent peaks in ES+, the compound with Rt 25.08 and MW 425.6 was suspected to be 2-(4-Chloro-3,5-dimethyl-1H-pyrazol-1-yl)-N-(3,5-difluoro-4-iodophenyl)acetamide with molecular formula $\text{C}_{13}\text{H}_{11}\text{ClF}_2\text{IN}_3\text{O}$ (Figure 3.9). The second compound with the next prominent peak in the ES+ zone was suspected to be methyl (3S,4R)-4-methoxy-3-[(2S)-2-[5-[4-[4-[2-[(3R)-3-(phenylcarbamoyl)-2-bicyclo[2.2.1]heptanyl]-3H-pyrrol-4-

yl]phenyl]phenyl]-1H-imidazol-2-yl]pyrrolidine-1-carbonyl]pentanoate (MW = 739.9; Rt = 15.44; MF= C₄₅H₄₉N₅O₅) (Figure 3.10).

In the ES-, the two suspected compounds are (5E)-3-[(4-bromophenyl)methyl]-5-[[4-[(2,4-dichlorophenyl)methoxy]-3,5-diiodophenyl]methylidene]imidazolidine-2,4-dione (MW= 784.006; Rt= 13.94; MF= C₂₄H₁₅BrCl₂I₂N₂O₃) (Figure 3.11), and 3,3'-{4-[(3β,5α)-8-Methylcholestan-3-yl]-1,1-butanediyl}bis(5-chloro-6-hydroxybenzoic acid) (MW= 783.903; Rt = 15.45; MF= C₄₆H₆₄Cl₂O₆) (Figure 12).

Table 3.1: Molecular ion (m/z) and fragment ion peaks

RT	MW	[M+H] ⁺ [M]	[M+NH ₄] ⁺	[M+Na] ⁺	[M-H] ⁻	[M+Cl] ⁻	[M+CH ₃ COO] ⁻
25.0 8	425. 6	426	443	448	424	460	484
15.4 4	739. 9	740.91	757.93	762.89	738.8 9	774.87	798.91
13.9 4	784	785.50	802.43	808.36	730.2 5	780.35	806.32
15.4 5	783. 9	784.50	799.32	804.28	760.2 0	811.17	825.23

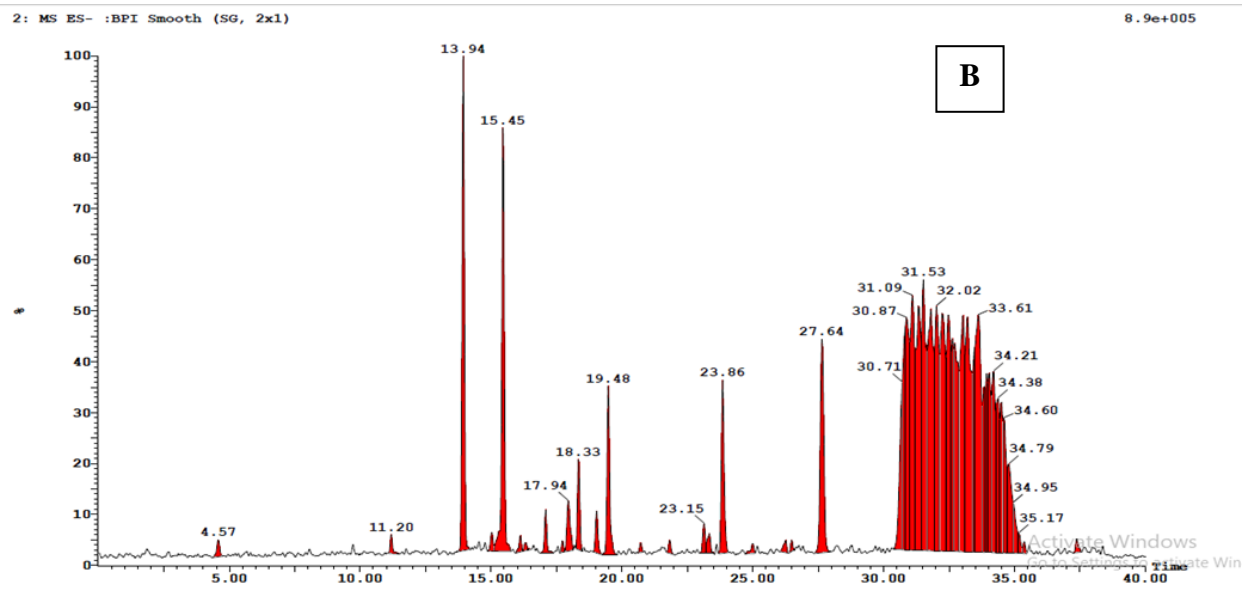
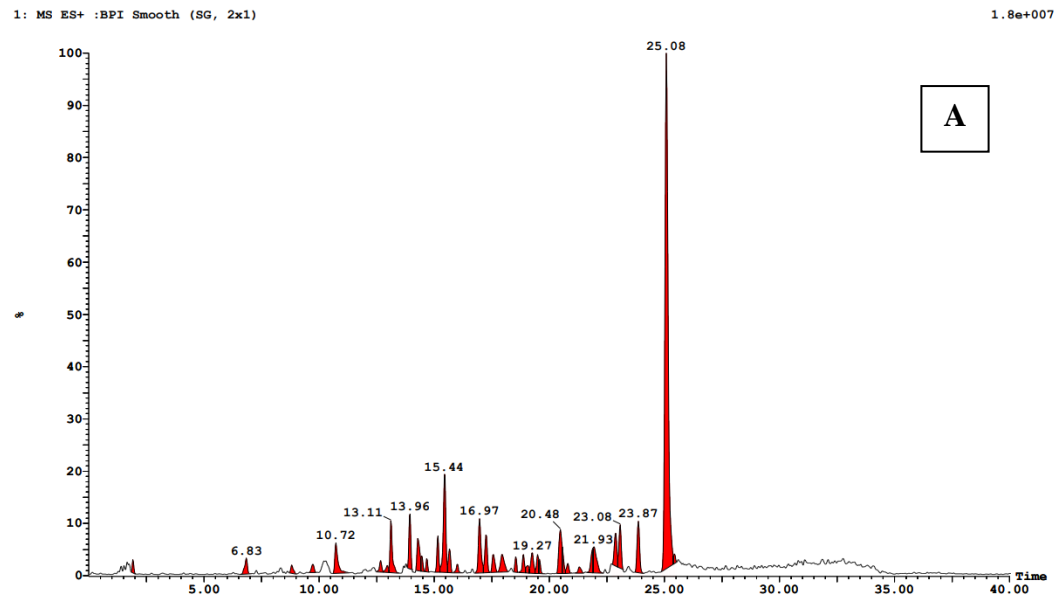


Figure 3.4: LC-MS Chromatogram of S-9-Ethyl Acetate Extract (A) ESI+; (B) ESI-

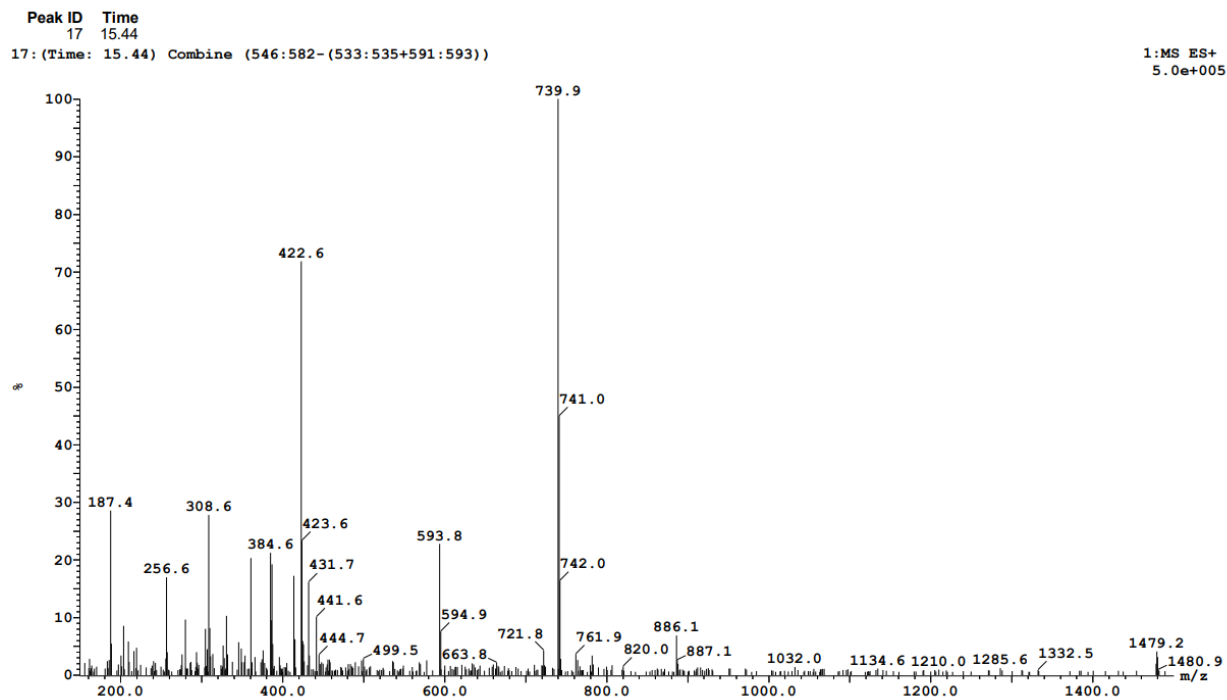


Figure 3.5: Mass fragmentation of S-9 ethyl acetate extract at 15.44 retention time in ES+

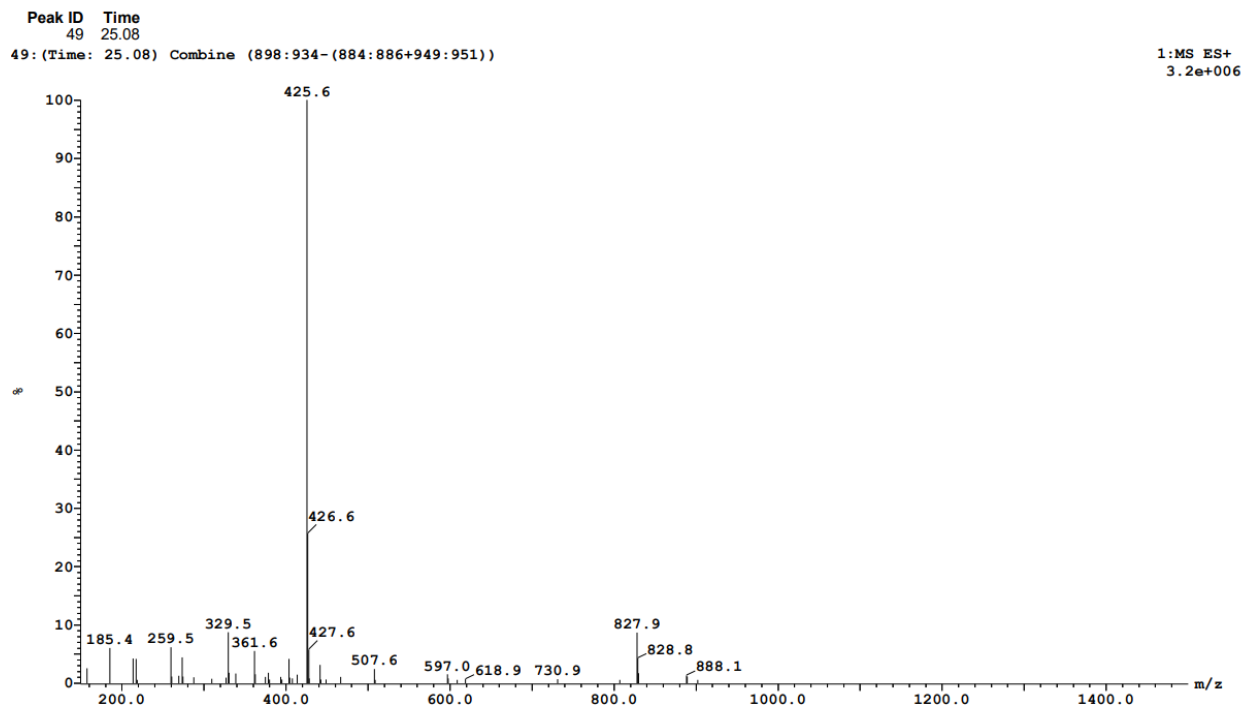


Figure 3.6: Mass fragmentation of S-9 ethyl acetate extract at 25.08 retention time in ES+

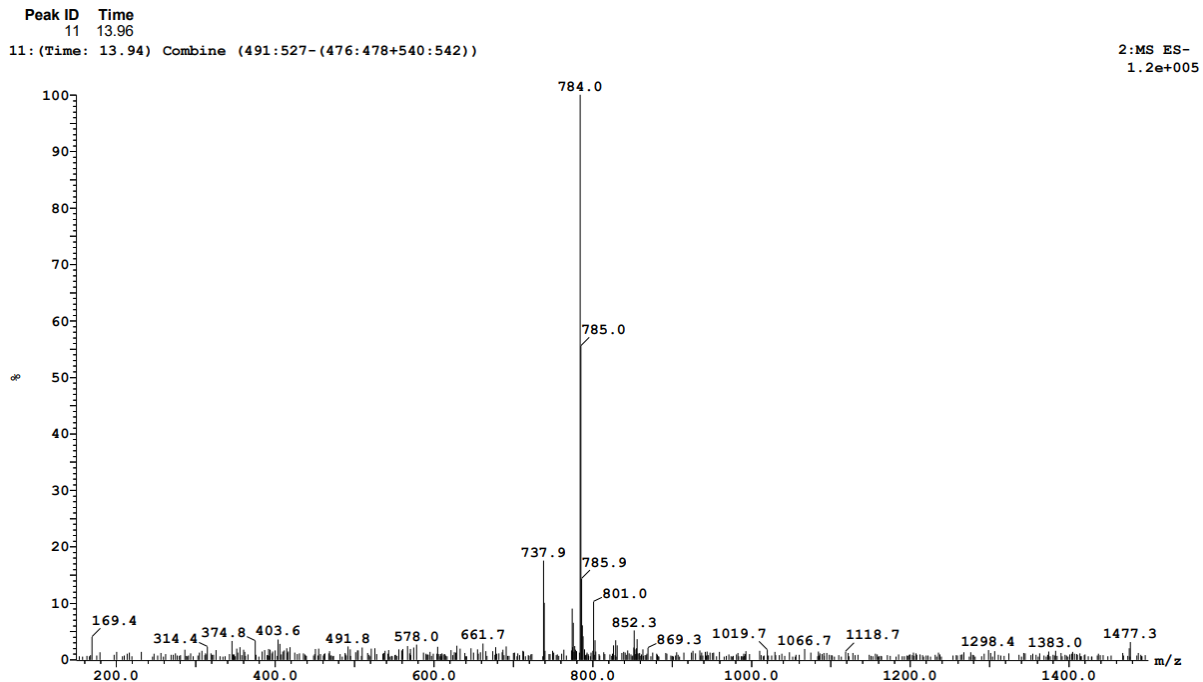


Figure 3.7: Mass fragmentation of S-9 ethyl acetate extract at 13.94 retention time in ES-

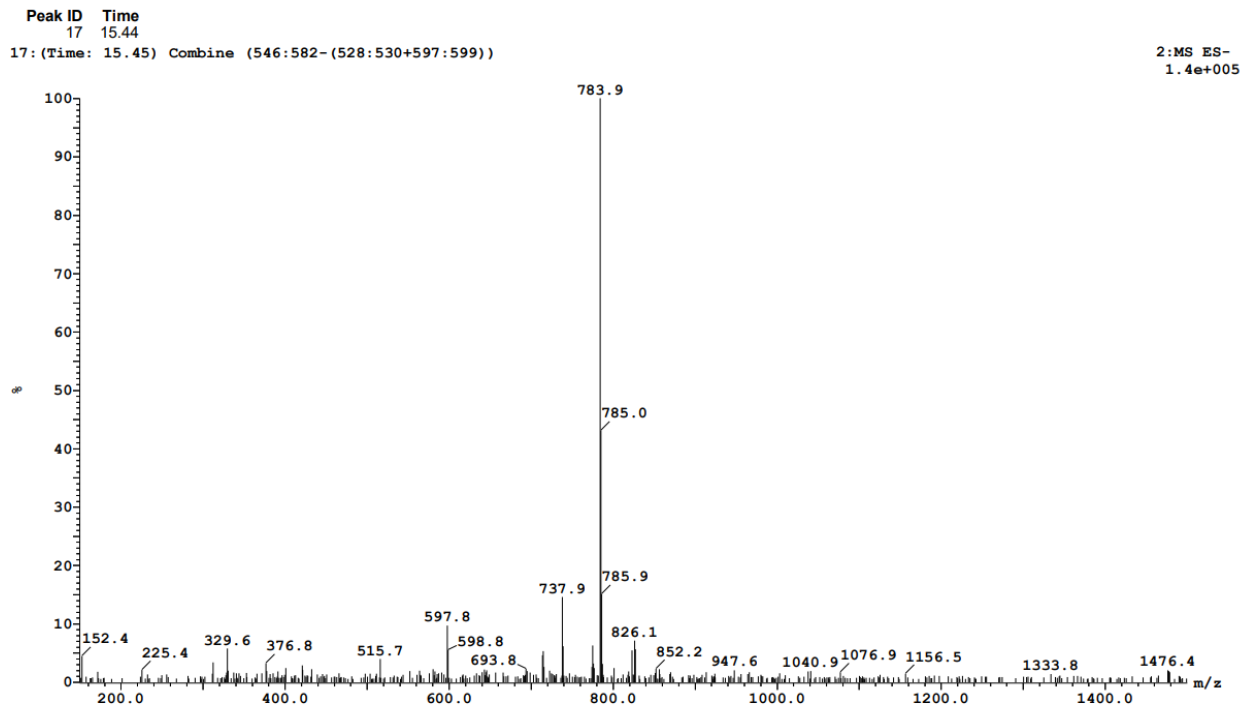


Figure 3.8: Mass fragmentation of S-9 ethyl acetate extract at 15.45 retention time in ES-

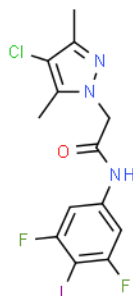


Figure 3.9: Molecular Structure of 2-(4-Chloro-3,5-dimethyl-1H-pyrazol-1-yl)-N-(3,5-difluoro-4-iodophenyl) acetamide

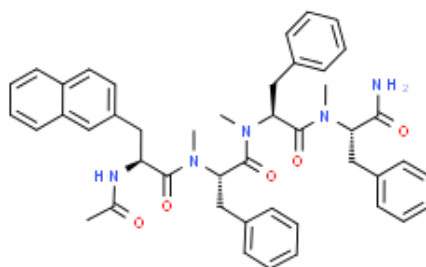


Figure 3.10: Molecular Structure of (2S,5S,8S,11S)-2,5,8-Tribenzyl-3,6,9-trimethyl-11-(2-naphthylmethyl)-4,7,10,13-tetraoxo-3,6,9,12-tetraazatetradecan-1-amide

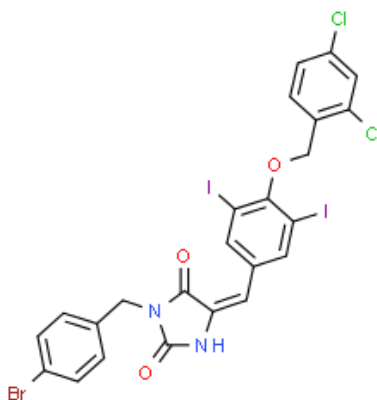


Figure 3.11: Molecular Structure of (5E)-3-[(4-bromophenyl)methyl]-5-[[4-[(2,4-dichlorophenyl)methoxy]-3,5-diiodophenyl]methylidene]imidazolidine-2,4-dione

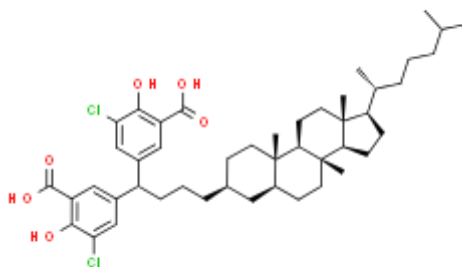


Figure 3.12: Molecular Structure of 3, 3'-{4-[(3 β ,5 α)-8-Methylcholestan-3-yl]-1,1-butanediyl}bis(5-chloro-6-hydroxybenzoic acid)

3.3.5 Proton nuclear magnetic resonance (^1H NMR) of purified bioactive compounds

S-9 strain was shown to contain an active ingredient against *Fusarium udum* during bioautography. The structure of this molecule was revealed using ^1H NMR analysis after it was purified using chromatographic techniques. The structure of compound, isolated from bioactive fraction of strain S-9 was elucidated from its ^1H NMR spectra 500 MHz, CDCl_3 (Figure 3.13), which showed characteristic methyl proton, $-\text{CH}_2\text{O}$ proton peak 4.15 ppm, $-\text{COCH}$ peak 2.04 ppm and $-\text{CH}_2$ peak 1.674 ppm (Table 3.2). The unknown compound was analysed using ^1H NMR which provided information on the number of different protons obtained by integrating the peak areas. Figure 3.13 depicts the ^1H NMR spectrum obtained with peak assignments of functional groups were listed. The peak showed nice triplet splitting pattern due to two neighbouring protons. From ^1H NMR, the reaction was successful and produced the desired product. During bioautography, the compounds present in the crude extract of strain S-9 were found active against *F. udum*.

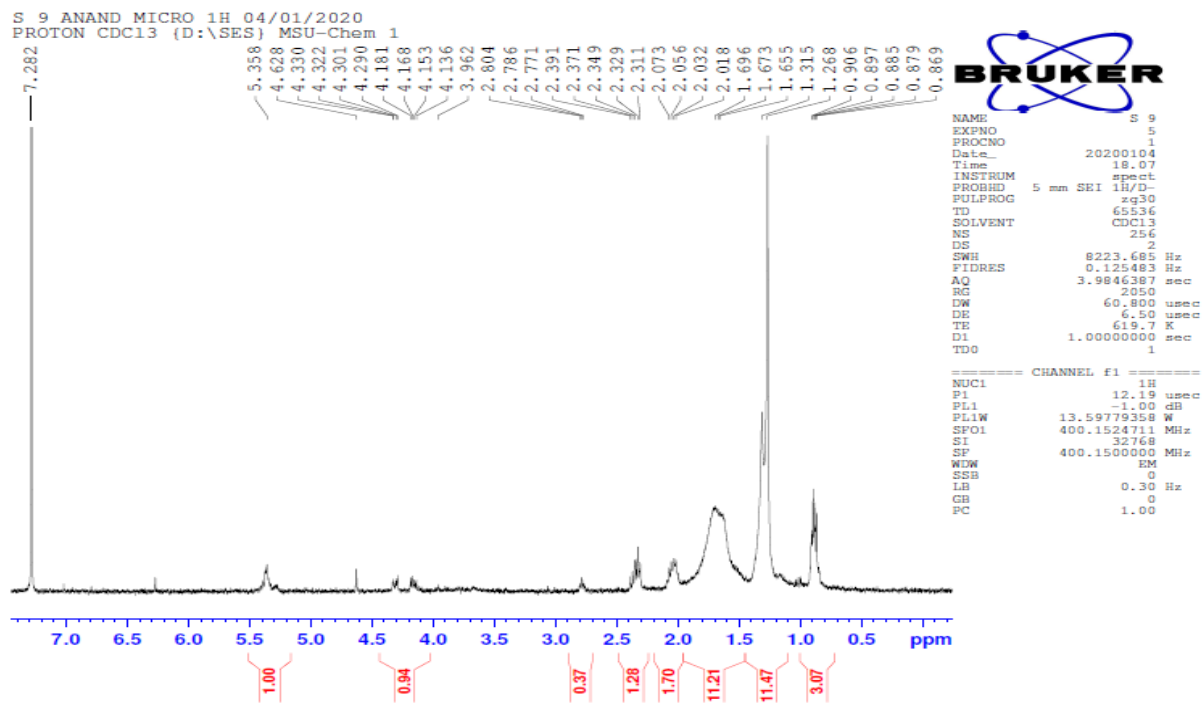


Figure 3.13: ^1H NMR Spectra of purified bioactive principle isolated from *Streptomyces* sp. S-9

Table 3.2: ^1H NMR Total Proton

Functional Groups	Total Proton(ppm)
-CH ₂ O	4.15
-COCH	2.04
-CH ₂	1.674
-CH ₂ OH	3.54

3.3.6 FTIR Analysis

The FTIR spectrum exhibited broad absorption peak between 1000-3000 cm^{-1} . The spectrum indicates that the compound had -C=O , -OC stretch, and -OH group. The presence of -CH_3 , CH_2 , C=O (lactone) stretch, -OH stretch, and ether and ester groups confirmed by the bands present in the region of 3019.03, 2927.85, 2855.61 cm^{-1} , 1735 cm^{-1} , 1215.64 cm^{-1} , and 1462 - 1022

cm⁻¹ respectively. The product obtained from the esterification reaction was characterized by IR spectroscopy (Figure 3.14). A weak band due to the O-H groups of ethanol was observed at ~ 3000 cm⁻¹; in this spectrum region, a series of bands appearing in the range of 2980 to 2850 cm⁻¹ were attributed to C-H stretching. The band occurring at 1735 cm⁻¹ was associated with the characteristic C=O stretching vibration of esters, while bands at 1190 cm⁻¹ were assigned to the C-O-C bending modes of the ester bond. Finally, those appearing at 1735 cm⁻¹ were assigned to the C-O stretch, confirming the formation of an unknown molecule.

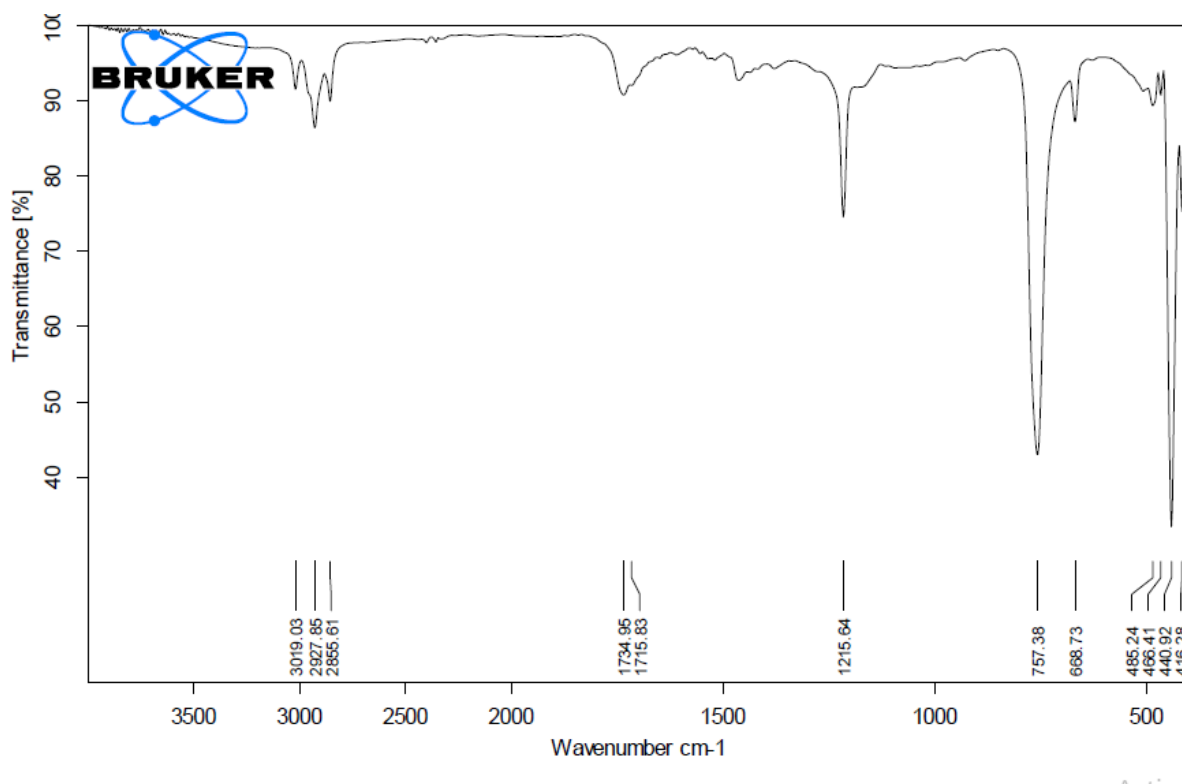


Figure 3.14: IR Spectral

3.4 Discussion

Crops suffered significant losses and rot due to plant fungal diseases (Duan et al., 2013). *Fusarium udum* wilt is a primary biotic factor that negatively impacts crop increase and yield in pigeon pea cultivation (30–60% of disease incidence occurs during the flowering and maturation stages) (Sharma et al., 2016). According to the accumulating evidence, actinobacteria are the most likely to produce small diversity molecules (Shivlata & Tulasi, 2015). Due to their

diverse growing circumstances and antagonistic activity, only a small number of Actinobacteria have been identified and utilized. Consequently, isolating and screening highly effective antagonistic Actinobacteria is essential for developing biocontrol agents. Several scientists have successfully employed protocols for identifying and purifying bioactive compounds utilized in this study during their research (Selvameenal et al., 2009; Solanki et al., 2015).

Currently, untargeted metabolomics analysis identifies metabolites primarily by mass-based searches followed by manual verification. First, the m/z value of the chemical ion of interest is queried against the databases (Cui et al., 2008; Wishart et al., 2009). The potential identifications of metabolites with molecular weights within a defined tolerance range of the query m/z value are retrieved from the databases. Then, actual chemicals corresponding to these tentative identifications are exposed to a tandem MS (MS/MS) experiment alongside the sample. The identities of the molecules can be confirmed by comparing the MS/MS spectra and retention times of the authentic compounds to those of the molecules of interest in the sample. Due to the availability of isomers and the low accuracy of mass spectrometers, putative identifications derived from mass-based searches are rarely unique (Kind & Fiehn, 2006). In our study, the compounds suspected to be present in the mixture in appreciable amounts have no information regarding their disease management implications. However, this has served as a basis for novel compound identification in *Streptomyces* sp. S-9.

The development of high-throughput metabolomics is driven by improvements in analytical technologies, such as nuclear magnetic resonance (NMR) spectroscopy and mass spectrometry (Chen et al., 2006). The ^1H NMR signal is formed by the migration of protons or other nuclei's magnetic moments in a magnetic field following their excitation by a high-frequency pulse (Silverstein & Bassler, 1962). A ^1H NMR spectrum depicts chemical shifts in parts per million (p.p.m., or the difference in hertz between a resonance frequency and a reference substance) versus signal intensities (Ernst et al., 1987). A metabolite detectable by ^1H NMR typically comprises one or more protons, with each proton producing one or more peaks. The chemical structure of a molecule reproduces and uniquely determines the number of peaks formed by a metabolite and their location and ratio of heights (C. Zheng et al., 2011).

FTIR is a useful tool that records or identifies different chemical bonds present in a molecule by producing an infrared absorption spectrum as a molecular fingerprint. The FTIR spectrum exhibited broad absorption peak between 1000-3000 cm^{-1} . This indicates the presence of several metabolites of interest; however, our compound is confirmed by LC-MS. Such instance where FTIR has been used for characterizing antimicrobial metabolite has been reported (Augustine et al., 2005; Dhanasekaran et al., 2008).